The Journal of Experimental Biology 213, 4213-4222
© 2010. Published by The Company of Biologists Ltd
doi:10.1242/jeb.048629

Photoentrainment in blind and sighted rodent species: responses to photophase light with different wavelengths

Abed E. Zubidat[1,*], Randy J. Nelson[2] and Abraham Haim[1,3]

[1]Department of Evolution and Environmental Biology, University of Haifa, Mount Carmel, Haifa 31905, Israel, [2]Departments of Neuroscience and Psychology, Ohio State University, Columbus, OH 43210, USA and [3]The Israeli Center for Interdisciplinary Research in Chronobiology, University of Haifa, Mount Carmel, Haifa 31905, Israel

*Author for correspondence (zubidat3@013.net)

Accepted 16 September 2010

SUMMARY

Our study examined the impact of daylight (photophase) wavelength on the photoentrainment sensitivity of two species with vastly different visual systems. Social voles (*Microtus socialis*) and 'blind' mole rats (*Spalax ehrenbergi*) were exposed to short-wavelength (479 nm) or long-wavelength (697 nm) light at an intensity of 293 μW cm^{-2}. Rhythms of urine production, urinary 6-sulfatoxymelatonin (6-SMT), urinary metabolites of adrenaline and cortisol, and oxygen consumption (VO_2) were used as markers for the sensitivity of the photoentrainment system. Significant 24-h rhythms were detected in all variables for both species under short-wavelength light, whereas ultradian rhythms of 12- or 8-h were detected under long-wavelength light. Wavelength inversely affected 6-SMT levels in *M. socialis* (negative correlation) and *S. ehrenbergi* (positive correlation). Increased levels of stress hormone metabolites were detected in *M. socialis* under the long-wavelength light whereas, in *S. ehrenbergi* elevated levels were secreted under short-wavelength light. Long-wavelength light increased VO_2 in *M. socialis* and decreased it in *S. ehrenbergi*; short-wavelength light elicited the opposite effects. Our results indicate that photophase wavelength is an integral light property for modulating photoperiodic responses in mammals, including visually challenged species. Finally, the spectral-induced differential responses between the two species potentially represent adaptive physiological flexibility in species with contrasting visual and habitat challenges.

Supplementary material available online at http://jeb.biologists.org/cgi/content/full/213/24/4213/DC1

Key words: cosinor analysis, masking, melanopsin, retinal photoreceptor, subterranean.

INTRODUCTION

The timing of the daily onset of light and dark as well as the annual cycle of changes in the daily ratio of light to dark hours provide the most reliable and enduring signals for accurately estimating time of day and time of year. The ability to track time of day and time of year allows individuals to anticipate predictable events such as night or winter and make appropriate physiological adjustments in anticipation of these upcoming environmental changes. Light information is received by distinct retinal photoreceptors, sent to the suprachiasmatic nucleus (SCN) and then projected by efferent connections to the pineal gland; the pineal comparably synthesizes and secretes melatonin during the dark period (scotophase) in diurnal and nocturnal mammals. The circulating melatonin rhythm is suggested to play a major regulating role in the mammalian photoentrainment system (Pévet et al., 2006; Pandi-Perumal et al., 2008; Zawilska et al., 2009). The mammalian retina presents two distinctive classes of photoreceptors: image-forming photoreceptors (IFPRs) and non-image-forming photoreceptors (NIFPRs). The IFPRs contain the visual pigments rhodopsin and opsins used for visual orientation, whereas NIFPRs include melanopsin and mainly function in circadian entrainment (Kavakli and Sancar, 2002; Güler et al., 2007; Güler et al., 2008). Several studies of humans and other animals with major deterioration of IFPRs have repeatedly demonstrated a severe lack of light perception for visual images, but not for seasonal or circadian entrainment (Lucas et al., 1999; Klerman et al., 2002; Van Gelder, 2005; Güler et al., 2008). The NIFPRs are intrinsically photosensitive, suggesting a crucial role for melanopsin in circadian entrainment (Berson, 2007; Graham et al., 2008; Hankins et al., 2008).

Microtus socialis (Pallas 1773) and *Spalax ehrenbergi* (Nehring 1898) represent extremes of ecological adaptation and visual capability. *M. socialis* is a semi-fossorial species with predominantly nocturnal activity patterns (Benjamini, 1989), but diurnal activity has also been recorded, mainly during winter (Harrison and Bates, 1991). The eyes of *M. socialis* are expected to express both IFPRs and NIFPRs, whereas *S. ehrenbergi* – an obligate subterranean species that spends its entire life underground – has eyes that have severely degenerated; the functioning remnants are concealed by skin and hardly any image-forming functions remain (Sanyal et al., 1990). However, several studies have reported that the vestigial eyes of *S. ehrenbergi* retain the ability to register light stimuli to adjust photoentrainable rhythms (Cooper et al., 1993; David-Gray et al., 1998; Cernuda-Cernuda et al., 2002). Daily rhythms of several behavioral and physiological functions that are responsive to light manipulations have been reported for *S. ehrenbergi* and *M. socialis*. However, these species display little overlap in their ranges of habitat and resource requirements [mole rats (Haim et al., 1983; Rado et al., 1991; Goldman et al., 1997; Avivi et al., 2004); voles (Banin et al., 1994; Haim et al., 2005; Zubidat and Haim, 2007; Zubidat et al., 2007; Zubidat et al., 2008)].

The effects of light with varying wavelength have been studied in several mammal species including rodents (Chávez et al., 2003; Aral et al., 2006) and species-specific spectral sensitivity modulation to different ecological niches has been suggested (Kumar and Rani,

1999; Reiter, 1994). Spectral sensitivity of *M. socialis* is expected to be in the blue to yellow range of the visible spectrum (≈430–530 nm), in common with most sighted mammalian species, including nocturnal rodents (Peichl, 2005; Bullough et al., 2006). In *S. ehrenbergi*, the vestigial retina is capable of receiving both blue-shifted wavelength light (rod photopigment), with a peak sensitivity of 497 nm (Janssen et al., 2000), and red-shifted wavelength light (cone photopigment), with a peak sensitivity of 530 nm (Janssen et al., 2003).

Recently, we have characterized the maximal effective photophase intensity for photoentrainment of daily rhythms in *M. socialis* and *S. ehrenbergi*, which approximated 293 μW cm^{-2} in the two species (Zubidat et al., 2009; Zubidat et al., 2010). Comparative studies between the two species revealed differences in their response to light intensity at a wavelength of 586 nm (Zubidat et al., 2009; Zubidat et al., 2010). Therefore, *M. socialis* and *S. ehrenbergi* were preferred for comparison because they are well-established animal models in the laboratory and their biological rhythms, including those of pineal melatonin production and secretion, are well characterized [*S. ehrenbergi* (Ben-Shlomo et al., 1996; Zubidat et al., 2009); *M. socialis* (Zubidat et al., 2007; Zubidat et al., 2009)]. Both species show seasonal changes in their thermoregulatory system entrained by changes in photoperiod [*S. ehrenbergi* (Haim et al., 1983); *M. socialis* (Banin et al., 1994)]. Although the two species belong to the suborder Myomorpha, they are at the opposite ends of the spectrum regarding their vision capabilities and requirements for habitat illumination. Additionally, *M. socialis* and *S. ehrenbergi*, as mentioned above, are classified as photoperiodic species and robustly react to light manipulations under laboratory conditions. Comparison of the circadian photoentrainment response to different photophase wavelength in these two species, therefore, is of great interest for detecting temporal variables and understanding their ecological consequences, and this was the goal of the present study.

We tested the effects of two monochromatic lights (short- and long-wavelength) at the maximal effective photophase intensity level on photoentrainment in *M. socialis* and *S. ehrenbergi*. Daily rhythms of urine production rate, urinary 6-sulfatoxymelatonin (6-SMT) excretion [the primary metabolite of melatonin in urine (Zawilska et al., 2009)], urinary metabolites of the stress hormones adrenaline (UMAdr) and cortisol (UMCort), and daily energy expenditure (DEE) [estimated by measuring the daily oxygen consumption (VO_2) rhythm] were evaluated under the designated monochromatic lights.

MATERIALS AND METHODS

Animals and housing

All experiments reported here were approved by the Ethics and Animal Care Committee of the University of Haifa (protocol no. 111/2008). Sixteen individual male *M. socialis* and 16 individual male *S. ehrenbergi*, 2n=60 karyotypic form (Nevo et al., 2001), were included in the experiments. *M. socialis* (four months of age, 45–63 g body mass) were obtained from our breeding colony at Oranim, University of Haifa, Kiryat Tivon, Israel. *S. ehrenbergi* (173–221 g body mass) were caught in cultivated fields from the Rehovot area (31°53′33.98″N, 34°48′40.58″E) during winter and spring. *M. socialis* and *S. ehrenbergi* were housed individually in clear plastic cages (43×23×26 cm) with wood shavings as bedding material. Food (Purina rodent pellets, Koffolk, Tel Aviv, Israel) and water (carrots as a water source) were provided *ad libitum*. All experiments were conducted in a climatic room maintained on short-day (SD) 8 h:16 h light:dark cycles (lights on from 08:00 to 16:00 h) at an ambient temperature (T_a) of 25±2°C and a relative humidity of 60%. Eight light fixtures (containing a single lamp) emitting either short- or long-wavelength monochromatic light (25 W; OSRAM, Molesheim, France) were located ~50 cm above the animal cage floor. All lamps were connected to a dimmer circuit (230 V AC; Fetaya Ltd, Rishon Le Zion, Israel) and were manually adjusted to 293 μW cm^{-2} maximal effective photophase intensity level (Zubidat et al., 2009; Zubidat et al., 2010). Although the 25 W monochromatic light bulbs used in our experiment emit heat, we have demonstrated that the expected heat emission from the lights did not affect the T_a inside the room or the body temperature of the animals (Zubidat et al., 2010). Photometric measurements were performed by a hand-held single fiber-optic spectrometer (AvaSpec-2048-FT-SDU, Avantes, Eerbeek, The Netherlands) while placing the light sensor directly beneath the lamp at the same distance between lamp and cage floor. The central wavelength of each monochromatic light was 479 nm for the short-wavelength lamps and 697 nm for the long-wavelength lamps.

Experimental protocol

Individuals of each species were randomly assigned to one of two experimental subgroups (N=8) and each was exposed, during the photophase, to either short- or long-wavelength monochromatic radiation at the maximal effective photophase intensity level of 293 μW cm^{-2} (Zubidat et al., 2009; Zubidat et al., 2010). Each group was maintained under experimental conditions for 3 weeks prior to data collection. This protocol was designed to evaluate the effect of these two monochromatic lights on urine production rate, melatonin level (by recording urinary 6-SMT), stress responses (assessed by UMAdr and UMCort release rates) and metabolic responses (by monitoring VO_2 levels).

Daily rhythms in urine production rate

Urine samples were collected at 4-h intervals over a 24-h period. At the end of the acclimation period, animals were transferred to special cages designed for urine collection (48×38×21 cm) with an electropolished AISI 304 stainless steel 0.7×0.7 cm mesh floor (TECNIPLAST S.p.A., Buguggiate, Italy). The screened urine was collected in a plastic tray beneath the cages and was transferred, at 4-h intervals, to Eppendorf tubes using disposable glass Pasteur pipettes, as previously described (Zubidat et al., 2009). Immediately after collection, each urine sample was weighed and fractionated into three equal parts for 6-SMT, UMAdr and UMCort level determinations. UMAdr aliquots were preserved at pH ≈ 3 by adding 2 to 3 drops of hydrochloric acid (0.1 mol l^{-1} HCl). All aliquots were stored in a freezer at –25°C until further analysis. The weight of each urine sample was obtained using an ED623S Satorius balance (±0.001 g; Goettingen, Germany) and its volume was estimated by assuming a specific gravity of 1 g ml^{-1}, as previously documented (Tendron-Franzin et al., 2004).

Hormone analysis

The immunoreactivity of urinary 6-SMT, UMAdr and UMCort was determined using immunoassay ELISA kits (IBL, Hamburg, Germany). All determinations were conducted in duplicate, as described previously (Zubidat et al., 2009; Zubidat et al., 2010). The absorbance of the immunoreaction was recorded spectrophotometrically at 450 nm in an automated ELISA reader (SunRise; Tecan, Mannedorf, Switzerland) and hormone concentrations were extrapolated by Magellan^{TM} data analysis software (Mannedorf, Switzerland). The intra- and interassay coefficients were 5.8–204 ng ml^{-1} (5.2–12.2%) and 12.4–220 ng ml^{-1}

(5.1–14.9%) for 6-SMT, respectively, and 5.4 and 12.8% for UMAdr and 3.5 and 6.9% for UMCort, respectively.

Daily rhythms in metabolic responses

Metabolic responses to photophase light with the different wavelengths were evaluated by monitoring VO_2 and calculating total DEE for both species. DEE levels were calculated from VO_2, assuming an energy ratio of 20.92 kJ per liter of O_2 utilized (Speakman, 2000). VO_2 uptake was simultaneously measured from five metabolic chambers (2 l in volume) using an open flow system as previously described (Zubidat et al., 2007). The differences in oxygen content between the influx and the efflux of dried air outflow from the metabolic chamber were monitored at 100 s time bins with a Servomex Xentra 4100 electrochemistry oxygen analyzer (Crowborough, UK) that interfaced with a computer utilizing Logal hardware and special software for viewing and analyzing the collected data (Wonderware InTouch 7,1,0,0; MODCON Systems, Tuchenhagen, Ireland). The metabolic chambers were placed inside a light-proof environmental incubator (LAB-Line EnvironETTE®, Dubuque, IA, USA) at a constant regulated T_a=25±2°C, relative humidity=60% and SD conditions. Monochromatic bulbs (N=4, 25 W; OSRAM) of either 479 nm (short-wavelength) or 697 nm (long-wavelength) were installed at about 30 cm above the chambers and mean irradiance level was adjusted to maximal effective photophase intensity level. During the VO_2 measurement, animals were provided pellets and carrots *ad libitum*. Tissue paper was added in order to absorb urine secretion.

Statistical analyses

All numerical data are presented as means ± 1 s.e.m. or 95% confidence intervals (CI) of the mean. Statistical significance for time, wavelength, and time × wavelength interaction effects on the experimental variables enumerated above, was determined using two-way mixed repeated-measures ANOVA (RM-ANOVA). This analysis was followed by one-way RM-ANOVA when significant effects of time or interaction were detected by the mixed model. *Post hoc* multiple comparisons were performed using a Bonferroni correction test for dependent data or a Student–Newman–Keuls (SNK) test for independent data. Student's *t*-tests were completed for all other mean comparisons between or within groups (e.g. day *vs* night, day/night differences, etc.), whereas Pearson correlation coefficients (r) were calculated to estimate a possible correlation between wavelength and the experiment variables, as appropriate.

Results were further analyzed for rhythmicity using the cosinor analysis (Nelson et al., 1979; Refinetti et al., 2007). The cosinor is a nonlinear reiteration least squares fitting method that generates the best cosine curve approximation of an entire set of data. Each set of time series data was fitted to the following cosine equation:

$$Y(t) = \text{Mesor} + \text{Amplitude} \times \cos\left(\frac{2\pi(t + \text{Acrophase})}{\tau}\right), \quad (1)$$

where $Y(t)$ is the variable value at time t of the equation defined by mesor (rhythm-estimated mean), amplitude (half the difference between the crest and trough of the cosine curve), acrophase (the crest time of the cosine curve with reference to local midnight, 00:00 h) and τ (the repeated period of the estimated wave). The τ of the best-fitted cosine curve was estimated using the Jankins–Watt autoperiodogram for data collected at regular intervals (Gouthiere et al., 2005). The cosinor analysis yields significant rhythms only when the variance accounted for by the cosine approximation at trial τ and by homogenous function (amplitude equal to zero) differs significantly according to the F-test of variance (P<0.05). The analysis also derives a measure of the predictability of the so-called percentage rhythm (PR), which indicates the percentage of variability in the entire data set that is accounted for by the cosine approximation. Statistical significance between derived rhythm estimates of two sets of data was calculated using the Bingham test (Bingham et al., 1982). All statistical analyses were performed using SPSS 15.0 for Windows (SPSS Inc., Chicago, IL, USA), except for the cosinor analysis, which was performed using the TSA-Time Series Analysis Serial Cosinor 6.3 software package (Expert Soft Technologie, Esvres, France).

RESULTS

Daily rhythms in urine production rate

Fig. 1 shows profiles of urine production rates over 24 h for the two species under photophase light with either short- or long-wavelength reflectance. For *M. socialis*, results of the 2-way mixed RM-ANOVA showed a significant time-related variation in urine production ($F_{2.89,40.39}$=6.67, P<0.001, N=16), significant differences among spectral groups ($F_{1,14}$=17.07, P<0.001, N=16) and significant interaction effects between time elapse and photophase spectral exposures ($F_{2.89,40.39}$=2.91, P<0.05, N=16). According to 1-way RM-ANOVA, however, a significant effect for time was detected for *M. socialis* exposed to short-wavelength, but not long-wavelength (see supplementary material Table S1), light. Mean urine volume levels calculated for *M. socialis* exposed to short-wavelength light (0.64±0.04 ml 100 g^{-1} h^{-1}) were significantly (P<0.001, N=16) higher when compared with those of the long-wavelength-exposed group (0.26±0.08 ml 100 g^{-1} h^{-1}). The day/night differences were significantly higher in the short-wavelength-exposed *M. socialis* than in the long-wavelength-exposed counterpart individuals, with highest values recorded during scotophase (Fig. 1) and acrophase occurring around midnight for the two spectral groups. Cosinor analysis revealed a significant 24-h rhythm with high PR (70%) for the short-wavelength-exposed *M. socialis* but not for the long-wavelength-exposed group. Amplitude and mesor levels differed significantly (P<0.05, N=16) between the two spectral groups, with much higher mesor under wider amplitude levels in the short-wavelength group (supplementary material Table S1).

In *S. ehrenbergi*, significant effects were also observed for time-related variation in urine production ($F_{6,84}$=8.33, P<0.0001, N=16) and interaction effects between time and spectral composition ($F_{6,84}$=5.01, P<0.0001, N=16). Furthermore, a split one-way RM-ANOVA for each of the two spectral groups indicated that urine production rates under either spectral exposure changed significantly with time (supplementary material Table S1). However, analysis of the spectral effects indicted that *S. ehrenbergi* exposed to short- and long-wavelength light produced urine daily at a comparable mean rate (~0.94 ml 100 g^{-1} h^{-1}; $F_{1,14}$=0.20, P>0.05). Complementarily, the cosinor approximation detected significant rhythms that oscillated at 24-h and 12-h τ in *S. ehrenbergi* exposed to short- and long-wavelength light during the photophase period, respectively (Fig. 1). The two rhythms had high PR levels (~50%) and differed neither by mesor nor by amplitude levels (supplementary material Table S1). The Pearson correlation test showed that urine production rates of *M. socialis* were inversely correlated with photophase wavelength (r=–0.71, P=0.0001, N=24). In contrast to *M. socialis*, the test did not detect any significant correlation between the two variables in *S. ehrenbergi* spectral groups (Table 1).

Daily rhythms in urinary 6-SMT

Daily (24-h) profiles of 6-SMT concentrations for both species are depicted in Fig. 2. The 2-way mixed RM-ANOVA indicated

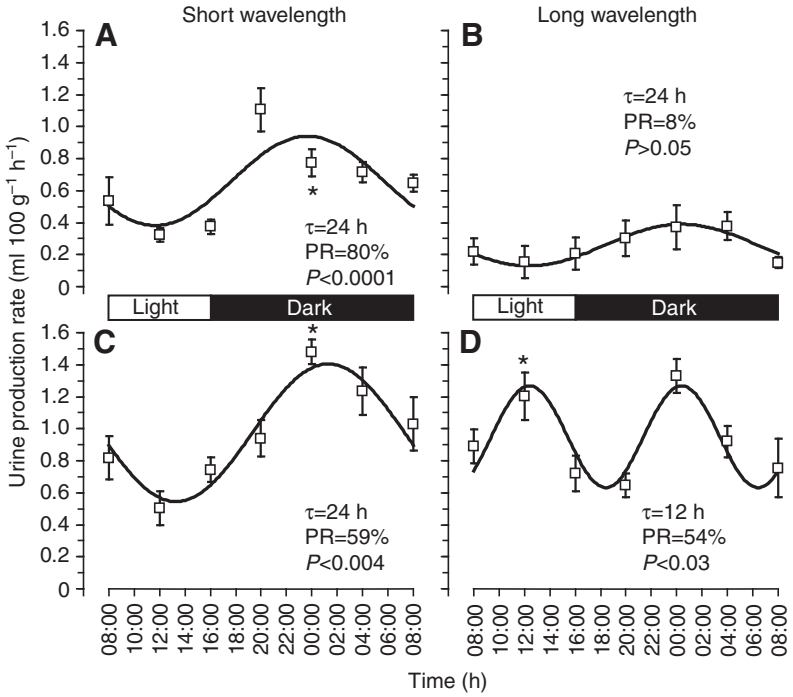

Fig. 1. Daily rhythms of urine production rate in *Microtus socialis* (A,B) and *Spalax ehrenbergi* (C,D) acclimated to photophase light with either short (479 nm) or long (697 nm) wavelength under short-day conditions (8 h:16 h light:dark, lights on from 08:00–16:00 h). Data are individual means (±s.e.m.) (ml 100 g^{-1} h^{-1}) of *N*=8; solid-line waves represent the best cosine curve approximation of the time series data. Percentage rhythm (PR), zero amplitude *P*-value and τ are given for each cosine curve. *M. socialis*: short wavelength: *, *P*<0.03 *vs* 12:00 and 16:00 h; *S. ehrenbergi*, short wavelength: *, *P*<0.001 *vs* 12:00 and 16:00 h; *S. ehrenbergi*, long wavelength: *, *P*<0.04 *vs* 20:00 h.

significant effects (*P*<0.0001) of time of day ($F_{3.22,38.6}$=10.28, *N*=14), spectrum levels ($F_{1,12}$=37.54, *N*=14) and the time × spectrum interaction ($F_{3.22,38.6}$=8.99, *N*=14) on urinary 6-SMT in *M. socialis*. Mean 6-SMT levels detected for short-wavelength-exposed *M. socialis* were 3.75±0.31 ng ml^{-1} whereas those for the long-wavelength-exposed group were only 1.79±0.07 ng ml^{-1}; these differences were statistically significant (*P*<0.001, *N*=14). The 6-SMT rhythms, when analyzed separately for time-related differences, showed significant variations in the short-wavelength-exposed *M. socialis* but not in the long-wavelength-exposed group (see supplementary material Table S2). Significant day/night differences (*t*=–6.44, d.f.=6, *P*=0.001, *N*=7) were detected only for *M. socialis* exposed to short-wavelength light, with acrophase levels occurring during scotophase at 02:49 h (Fig. 2). Cosinor analysis detected a 24-h rhythm in urinary 6-SMT concentrations for short-wavelength-exposed *M. socialis* and an ultradian rhythm with 8-h τ for the long-wavelength-exposed group, both of which were statistically significant with high PR levels (68 and 48%, respectively; supplementary material Table S2). Mesor and amplitude comparisons detected no significant differences in the levels of the two estimates between short- and long-wavelength-exposed *M. socialis* (*P*>0.05).

Similar to *M. socialis*, urinary 6-SMT levels of *S. ehrenbergi* showed significant (*P*<0.0001) effects of time of day ($F_{6,72}$=10.20, *N*=14), spectrum ($F_{1,12}$=87.03, *N*=14) and the time × spectrum interaction ($F_{6,72}$=6.79, *N*=14). In contrast to *M. socialis*, *S. ehrenbergi* urinary 6-SMT manifested higher values during long-wavelength light exposure than under short-wavelength conditions (3.16±0.15 and 1.25±0.14 ng ml^{-1}, respectively). The time-related variation in 6-SMT levels was also confirmed separately by the 1-way RM-ANOVA for both spectral groups of *S. ehrenbergi* (supplementary material Table S2). Significant day/night differences were only observed in the long-wavelength-exposed group. The cosinor analysis revealed clear rhythms, which oscillated with 24-h

Table 1. Pearson correlation and mean ± s.e.m. levels of physiological functions in two rodent species, *Microtus socialis* and *Spalax ehrenbergi*, under different spectral compositions

Variable	Species	Blue light (SW; 479 nm)	Yellow light (586 nm)	Red light (LW; 697 nm)	Pearson correlation		
					N	*P*	*r*
Urine production (ml 100 g^{-1} h^{-1})	*M. socialis*	0.64±0.04	0.45±0.09	0.26±0.08	24	0.0001	–0.71
	S. ehrenbergi	0.92±0.07	0.55±0.04	0.96±0.06	22	0.41	–0.19
6-SMT (ng ml^{-1})	*M. socialis*	3.75±0.3	1.7±0.1	1.79±0.07	21	0.0001	–0.75
	S. ehrenbergi	1.25±0.1	0.97±0.11	3.16±0.15	20	0.0001	0.78
UMAdr (pg ml^{-1} g^{-1})	*M. socialis*	175.66±9.4	201±17	256.98±29	21	0.002	0.63
	S. ehrenbergi	177.38±24	85±9	68.64±12.36	21	0.0001	–0.7
UMCort (pg ml^{-1} g^{-1})	*M. socialis*	33.9±4.56	64±13	62±1.8	21	0.03	0.48
	S. ehrenbergi	49.19±2.42	27±1.76	11.66±1.50	21	0.0001	–0.95
Total DEE (kJ g^{-1} day^{-1})	*M. socialis*	0.98±0.08	0.81±0.18	1.34±0.06	24	0.04	0.38
	S. ehrenbergi	1.53±0.09	1.09±0.06	0.98±0.08	24	0.001	–0.71

Data were adapted from our previous studies (Zubidat et al., 2009; Zubidat et al., 2010).
Correlations were performed between photophase wavelength levels and individual 24-h means.
6-SMT, 6-sulfatoxymelatonin; UMAdr and UMCort, urinary metabolites of adrenaline and cortisol, respectively; DEE, daily energy expenditure; SW, short wavelength; LW, long wavelength.

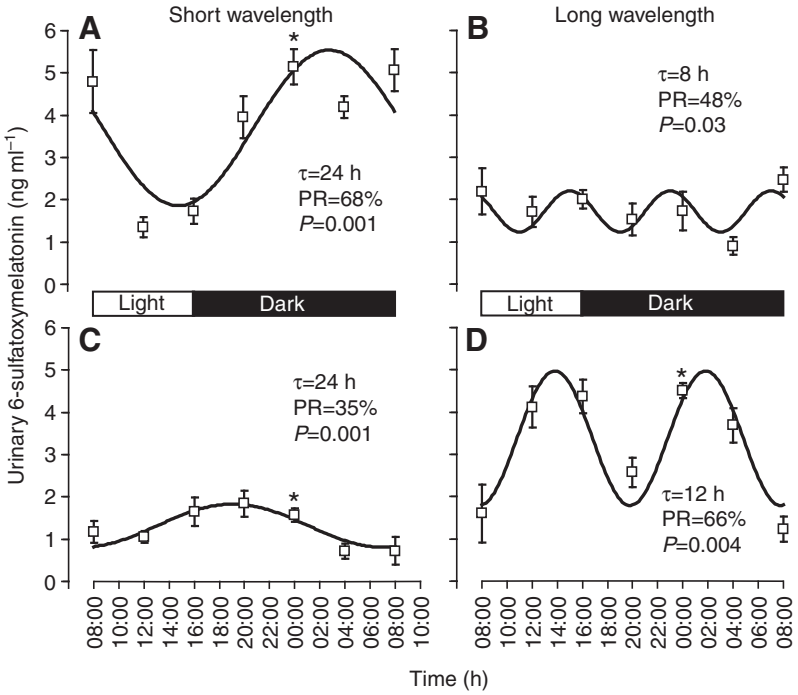

Fig. 2. Daily rhythms of urinary 6-sulfatoxymelatonin (6-SMT) release in *Microtus socialis* (A,B) and *Spalax ehrenbergi* (C,D) acclimated to photophase light with either short (479 nm) or long (697 nm) wavelength under short-day conditions (see Fig. 1 legend). Data are individual means (±s.e.m.) (ng ml^{-1}) of N=7 and solid-line waves represent the best cosine curve approximation of the time series data. Percentage rhythm (PR), zero amplitude P-value and τ are given for each cosine curve. *M. socialis*, short wavelength: *, P<0.03 *vs* 12:00 and 16:00 h; *S. ehrenbergi*, short wavelength: *, P<0.03 *vs* 04:00 h; *S. ehrenbergi*, long wavelength: *, P<0.02 *vs* 20:00 h.

(PR=61%) and 12-h (PR=66%) τ for short- and long-wavelength-exposed *S. ehrenbergi*, respectively (Fig. 2). The acrophase levels of the 24-h rhythm occurred during scotophase at 19:04 h and, in the ultradian rhythms, the first acrophase occurred during scotophase at 01:48 h. Moreover, the short-wavelength-exposed *S. ehrenbergi* displayed significantly lower mesor and amplitude levels compared with those calculated for their long-wavelength-exposed counterparts. In *M. socialis*, a significant negative correlation between wavelength and 6-SMT concentration (r=–0.75, P=0.0001, N=21) was observed. In contrast with *M. socialis*, the analysis detected a high positive relation between the two variables for *S. ehrenbergi* (r=0.75, P=0.0001, N=20; Table 1).

Daily rhythms in urinary metabolites of stress hormones

UMAdr

According to the 2-way mixed RM-ANOVA analysis, there were significant effects (P<0.0001) of time of day ($F_{2.85,34.16}$=16.18, N=7), photophase wavelength ($F_{1,12}$=13.3, N=14) and the time × wavelength interaction ($F_{2.85,34.16}$=7.23, N=14) on daily rhythms of UMAdr in *M. socialis*. UMAdr mean levels in the long-wavelength group (256.98±29.38 pg ml^{-1} g^{-1}) were significantly (P<0.003, N=14) higher than those in the short-wavelength group (175.66±9.40 pg ml^{-1} g^{-1}). When each photophase wavelength group was analyzed separately for the effect of time, a significant effect of time elapsed on UMAdr levels was established for both the short- and long-wavelength-exposed animals (see supplementary material Table S3). In the short-wavelength-exposed group, there were clear day/night differences in UMAdr levels, with higher levels occurring during photophase (t=3.97, d.f.=6, P<0.01, N=7). However, in the long-wavelength-exposed group, there was no significant day/night difference. Clear daily rhythms in UMAdr concentrations with τ of 24 h were observed in the two wavelength groups and, in both groups, high PR levels (~50%) were estimated (Fig. 3). Under short-wavelength conditions, the acrophase levels were recorded early in scotophase at 17:28 h; acrophase levels were delayed by ~4 h in the long-wavelength group. Mesor and amplitude levels calculated for the long-wavelength-exposed animals were manifestly higher compared with those exposed to short-wavelength light (supplementary material Table S3).

In *S. ehrenbergi*, significant effects of time ($F_{6,72}$=2.85, P<0.02, N=14), spectrum ($F_{1,12}$=15.57, P<0.002, N=14) and the time × spectrum interaction ($F_{6,72}$=2.30, P<0.05, N=14) on UMAdr levels were detected. Mean levels calculated for the short-wavelength-exposed (177.38±24.64 pg ml^{-1} g^{-1}) animals were significantly (P<0.002, N=14) elevated compared with those calculated for the long-wavelength-exposed animals (68.64±12.36 pg ml^{-1} g^{-1}). Consistently, the one-way RM-ANOVA split analysis showed significant time-related variations in UMAdr levels for the two wavelength groups (supplementary material Table S3). However, the paired t-test comparison detected significant day/night differences in the long-wavelength-exposed group (t=2.81, d.f.=6, P<0.05, N=7), but no clear differences were established for the other group. In the short-wavelength group, the cosinor analysis detected a complex rhythm consisting of two cyclic components with τ of 24 and 8 h and PR levels of 24 and 39%, respectively. In the long-wavelength-exposed group, the cosinor analysis detected a significant rhythm that oscillated at a τ of 24 h and exhibited higher PR levels (66%) compared with the short-wavelength group (Fig. 3). Furthermore, mesor levels of short-wavelength-exposed *S. ehrenbergi* were significantly higher than those of the long-wavelength group. The acrophase of the 24-h and the first acrophase of the 8-h components in the short-wavelength-exposed *S. ehrenbergi* occurred during scotophase, whereas the acrophase of the 24-h rhythms in the long-wavelength group occurred at the end of the photophase period (supplementary material Table S3). Finally, the Pearson correlation test showed significant positive (r=0.63, P<0.002, N=21) and negative (r=–0.70, P<0.0001, N=21) relationships between wavelength and UMAdr levels in the short- and long-wavelength-exposed *S. ehrenbergi*, respectively (Table 1).

UMCort

In *M. socialis*, the release profile of UMCort exhibited significant effects of time of day ($F_{3.11,37.25}$=3.04, P<0.04, N=14), spectrum ($F_{1,12}$=32.83, P<0.0001, N=14) and the time × spectrum interaction

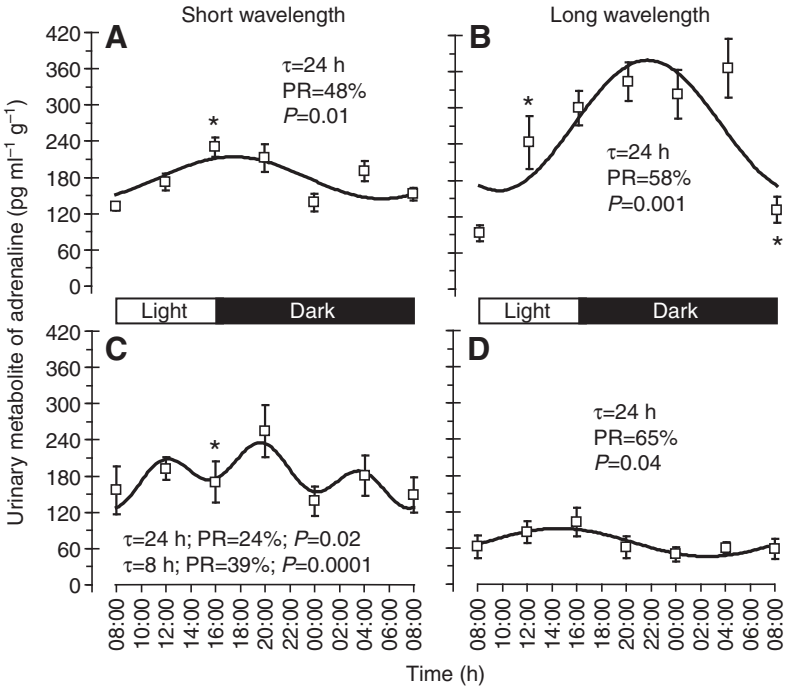

Fig. 3. Daily rhythms of urinary metabolites of adrenaline (UMAdr) release in *Microtus socialis* (A,B) and *Spalax ehrenbergi* (C,D) acclimated to photophase light with either short (479 nm) or long (697 nm) wavelength under short-day conditions (see Fig. 1 legend). Data are individual means (±s.e.m.) (pg ml^{-1} g^{-1}) of N=7 and solid-line waves represent the best cosine curve approximation of the time series data. Percentage rhythm (PR), zero amplitude P-value and τ are given for each cosine curve. *M. socialis*, short wavelength: *, P<0.04 *vs* 00:00 h; *M. socialis*, long wavelength: *, P<0.03 *vs* all time points; *S. ehrenbergi*, long wavelength: *, P<0.01 *vs* 08:00 h.

($F_{3.11,37.25}$=4.73, P<0.006, N=14). Consequently, mean UMCort levels excreted under long-wavelength light were significantly higher (P<0.0001, N=14) compared with those measured under short-wavelength light. The daily UMCort profile, when subjected to a one-way RM-ANOVA analysis, showed significant time related-variations only under the long-wavelength photophase exposure (see supplementary material Table S4). Unlike the UMCort daily rhythm under short-wavelength-exposed *M. socialis*, which is characterized by significant day/night differences (t=–4.08, d.f.=6, P<0.005, N=7), with increased levels at night, the hormone-release profile under long-wavelength-exposed *M. socialis* exhibited no evident day/night differences (Fig. 4). The cosinor analysis detected significant rhythms under the two wavelength exposures, but while the rhythm under the long-wavelength condition oscillated with a 24-h τ, that under short-wavelength-conditions oscillated with a notable shorter τ of 12.9 h. Additionally, the acrophase for the two rhythms was early in the morning at 08:02 h (short-wavelength) and 10:04 h (long-wavelength), and significantly differed by their mesor levels (the rhythm-estimated means) (Table S4).

In contrast to *M. socialis*, UMCort daily levels in *S. ehrenbergi* were not affected by time of day ($F_{2.82,33.81}$=2.26, P>0.05) or by the time × spectrum interaction ($F_{2.82,33.81}$=1.86, P>0.05). However, there was a significant effect of wavelength manipulation on the UMCort release profile ($F_{1,12}$=173.63, P<0.0001, N=14). Mean levels of UMCort in the short-wavelength-exposed *S. ehrenbergi* (49.19±2.42 pg ml^{-1} g^{-1}) were significantly higher (P<0.0001, N=14) compared with those of the long-wavelength-exposed group (11.66±1.50 pg ml^{-1} g^{-1}). The 1-way RM-ANOVA revealed obvious daily variations in UMCort levels only under long-wavelength light conditions, with significantly increased release (t=–2.92, d.f.=6, P<0.05, N=7) during scotophase (Table S4). The rhythm spectral analysis estimated a significant 24-h rhythm under long-wavelength but not under short-wavelength light (Fig. 4). All of the calculated rhythm variables (mesor, amplitude and acrophase) were significantly different between the two spectral groups (supplementary material Table S4). In contrast to the significant positive correlation (r=0.48, P<0.05, N=21) between UMCort levels and wavelength in *M. socialis*, the variables were negatively correlated in *S. ehrenbergi* (r=–0.95, P<0.0001, N=21; Table 1).

Daily rhythms in metabolic response

A representative profile of VO_2 rates over 48 h for both species is depicted in Fig. 5. VO_2 rates for *M. socialis* display significant daily temporal variation ($F_{48,672}$=4.87, P<0.0001, N=16) and were significantly affected by spectral composition ($F_{1,14}$=39.04, P<0.0001) and the time × spectrum interaction ($F_{48,672}$=2.81, P<0.0001, N=16). Mean rates under short-wavelength light (1.84±0.08 ml O_2 100 g^{-1} h^{-1}) were significantly lower (P<0.001, N=16) compared with those detected under long-wavelength light (2.71±0.12 ml O_2 100 g^{-1} h^{-1}). Individuals under the two spectral compositions also showed significant time-related variation in VO_2 rates when subjected to one-way RM-ANOVA analysis (see supplementary material Table S5). However, the paired t-test analysis failed to establish clear day/night differences in VO_2 rates under the two wavelengths. A significant 24-h rhythm was detected by the spectral analysis for *M. socialis* in the short-wavelength light experiment (PR=73%, P<0.001, N=8). Two harmonics of the 24-h rhythm were significant (24 and 12 h, PR=43 and 23%, P<0.05 and 0.01, N=8, respectively) in the model describing the VO_2 pattern in long-wavelength-exposed *M. socialis* (Fig. 5). However, the rhythm of long-wavelength-exposed *M. socialis* oscillated with high amplitude (mean±95% CI, 0.37±0.25–0.48 ml O_2 100 g^{-1} h^{-1}) and higher mesor levels in comparison with those of the short-wavelength-exposed group (supplementary material Table S5). Total DEE levels calculated for the short-wavelength-exposed *M. socialis* (0.98±0.08 kJ g^{-1} day^{-1}) were lower compared with those of the long-wavelength-exposed group (1.34±0.06 kJ g^{-1} day^{-1}) and these differences were significant (t=–3.66, d.f.=14, P<0.05, N=16; Table 1).

In *S. ehrenbergi*, VO_2 rates were significantly (P<0.0001) affected by time of day ($F_{48,672}$=3.97, N=16) and spectrum ($F_{1,14}$=25.14,

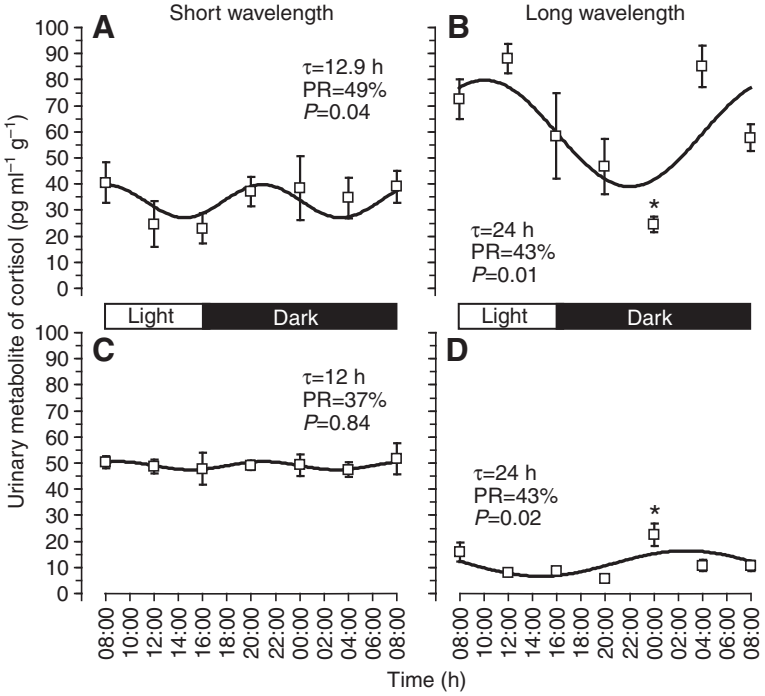

Fig. 4. Daily rhythms of urinary metabolites of cortisol (UMCort) release in *Microtus socialis* (A,B) and *Spalax ehrenbergi* (C,D) acclimated to photophase light with either short (479 nm) or long (697 nm) wavelength under short-day conditions (see Fig. 1 legend). Data are individual means (±s.e.m.) (pg ml^{-1} g^{-1}) of N=7 and solid-line waves represent the best cosine curve approximation of the time series data. Percentage rhythm (PR), zero amplitude P-value and τ are given for each cosine curve. *M. socialis*, long wavelength: *, P<0.001 *vs* 12:00 and 04:00 h; *S. ehrenbergi*, long wavelength: *, P<0.05 *vs* 12:00, 16:00 and 20:00 h.

N=16). Conversely, the 2-way mixed RM-MANOVA did not detect significant time × spectrum interaction effects on VO_2 daily rates ($F_{4,672}$=1.33, P>0.05, N=16). In contrast to *M. socialis*, the mean rate of VO_2 recorded for short-wavelength-exposed *S. ehrenbergi* (3.14±0.18 ml O_2 100 g^{-1} h^{-1}) was significantly elevated (P<0.0001) compared with that calculated for the long-wavelength-exposed group (1.19±0.16 ml O_2 100 g^{-1} h^{-1}). When the two spectral group rhythms were analyzed separately for time-related differences, a marked daily variation was detected for both groups (supplementary material Table S5). The cosinor analysis revealed a significant (PR=45%, P<0.0001, N=8) 24-h rhythm in *S. ehrenbergi* exposed to short-wavelength light. In the group exposed to long-wavelength light, the spectral analysis illustrated a compound rhythm consisting of two harmonics (24- and 12-h τ) (PR=30 and 22%, P<0.0001, N=8, respectively; Fig. 5). All rhythms displayed late nocturnal acrophases (after midnight) and similar amplitudes (~0.35 ml O_2 100 g^{-1} h^{-1}), except for the 24-h component of the compound rhythm under long-wavelength light (0.52 ml O_2 100 g^{-1} h^{-1}). Additionally, the 24-h rhythm detected for the short-wavelength-exposed *S. ehrenbergi* significantly (P<0.05, N=16) increased the mesor level (3.13 ml O_2 100 g^{-1} h^{-1}) compared with that calculated for the long-wavelength-exposed group (1.92 ml O_2 100 g^{-1} h^{-1}; supplementary material Table S5). The calculated total DEE levels for the short-wavelength-exposed *S. ehrenbergi* were clearly elevated (1.53±0.09 kJ g^{-1} day^{-1}) compared with those calculated for the long-wavelength-exposed group

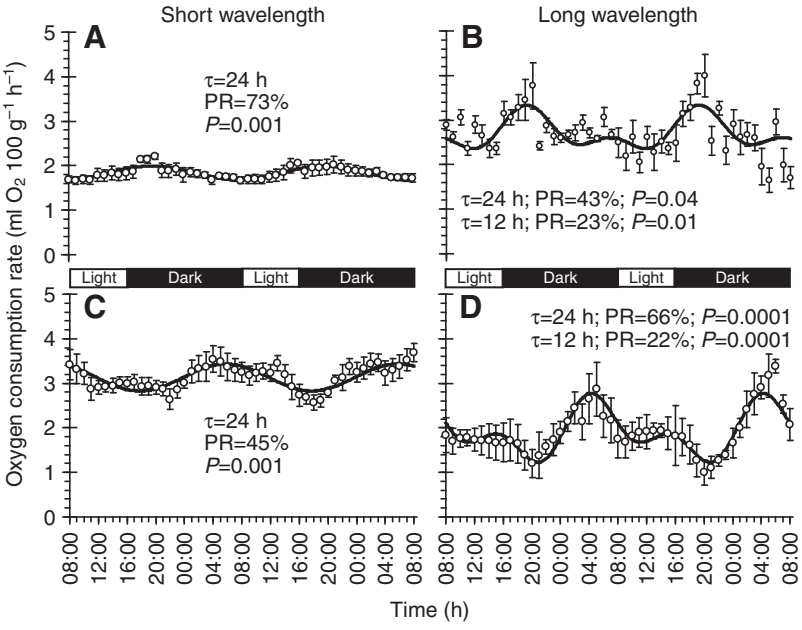

Fig. 5. Daily rhythms of oxygen consumption (VO_2) levels in *Microtus socialis* (A,B) and *Spalax ehrenbergi* (C,D) acclimated to photophase light with either short (479 nm) or long (697 nm) wavelength under short-day conditions (see Fig. 1 legend). Data are individual means (±s.e.m.) (ml 100 g^{-1} h^{-1}) of N=8 and solid-line waves represent the best cosine curve approximation of the time series data. Percentage rhythm (PR), zero amplitude P-value and τ are given for each cosine curve.

(0.98±0.08 kJ g^{-1} day^{-1}; Table 1). Finally, significant positive and negative correlations (r=0.38, P<0.05, N=24 and r=0.71, P<0.001, N=24) were detected between photophase wavelength and total DEE levels in short- and long-wavelength-exposed groups, respectively (Table 1).

DISCUSSION

Daily rhythms in urine production and 6-SMT levels

Renal rhythmic function of the two species in the present study appears to be modulated by the spectral composition of photophase light. *M. socialis* appears to be most sensitive to light with short-wavelength radiation. A distinct rhythm in urine production was only detected under short-wavelength monochromatic light whereas, under long-wavelength light, urine production displayed low and statistically insignificant amplitude. In contrast to *M. socialis*, *S. ehrenbergi* was equally sensitive to both short- and long-wavelength light, but the rhythm frequency of urine production was inversely related to wavelength exposure (Fig. 1). These results might reflect an ultradian character of the endogenous rhythm in *S. ehrenbergi*, which lives in virtually complete darkness in its natural subterranean habitat.

Our results demonstrated that the τ rhythm of 6-SMT was affected by photophase wavelength. Short-wavelength exposure shortened τ of the two species (8 and 12 h for *M. socialis* and *S. ehrenbergi*, respectively) compared with the predominant 24 h τ detected under the long-wavelength condition (Fig. 2). Dual-model profiles of melatonin levels throughout the day with early and late scotopic acrophases have been repeatedly documented in the scientific literature for humans and other animals, including *S. ehrenbergi* (Arendt, 1985; Wehr et al., 1995; Nakahara et al., 2003; Zubidat et al., 2009). Ultradian rhythms may be controlled by at least two endogenous oscillators that aim to enhance individual survival in natural habitats (Daan and Aschoff, 1982; Gerkema et al., 1990).

Our results showed contrasting responses between the two species in terms of mean 6-SMT levels under the varying photophase wavelength. In *M. socialis*, the amplitude, mesor and day/night differences of 6-SMT were most notable in response to short-wavelength exposure whereas, in *S. ehrenbergi*, augmented responses were evident under long-wavelength exposure (Table 1) (supplementary material Table S2). These results suggest that short-wavelength monochromatic light provides the optimal entrainment wavelength for regulating melatonin rhythm in the visually intact *M. socialis*. This suggestion is consistent with previous data for action spectra in sighted rodents, which have shown that blue light shifted the action sensitivity for circadian photoentrainment (Peichl, 2005; Bullough et al., 2006). Conversely, 'blind' *S. ehrenbergi* have a much lower sensitivity to wavelength in which the optimal entrainment for melatonin rhythms is achieved under long-wavelength monochromatic daytime light.

The optimal wavelength sensitivity for *M. socialis* and *S. ehrenbergi* established here likely corresponds to the light characteristics in their natural habitats. *M. socialis* remains concealed underground during the day and emerges to forage at night. Additionally, *M. socialis* can shift to diurnal activity during relatively cold and cloudy winter days (Harrison and Bates, 1991). However, *S. ehrenbergi* demonstrates a very different life history strategy; virtually all of their life is spent completely underground. Thus, exposure to aboveground illumination conditions is rare (Nevo, 1999). Consequently, the sensitivity to short-wavelength light for *M. socialis* is likely to be adequate for visual and nonvisual perception of surface light with high-power spectral composition. By contrast, *S. ehrenbergi* exhibits elevated sensitivity to long-wavelength light, which is appropriate for the faint spectral power of its underground burrows.

Daily rhythms in urinary metabolites of stress hormones

In the present study, the stress responses of *M. socialis* correlated significantly and inversely with wavelength; higher levels of UMAdr and UMCort were released in response to short-wavelength light. An opposite correlation was revealed for *S. ehrenbergi*. Our results confirm and extend previous findings that acute alteration in the properties of the light input into the visual system acts as a stressor. UMAdr and UMCort metabolites were markedly elevated in *M. socialis* in response to light-at-night (LAN) exposure (Zubidat et al., 2007) and in both species in response to photophase light with extreme intensities – low and high (Zubidat et al., 2010). Neither the short- nor the long-wavelength illuminations are typical for *S. ehrenbergi* or *M. socialis*, respectively. The manifested release of the stress hormones reflects an acute activation of the sympatho-adrenomedullaty (SAM) system and the hypothalamic–pituitary–adrenocortical (HPA) axis. Challenges (e.g. cold exposure, hypoglycemia, acute immobilization, etc.) that might compromise homoeostasis are completely associated with the activation of the SAM system and the HPA axis (Dunn and Swiergiel, 2008; Goldstein and Kopin, 2008). Thus, our results indicate that stress systems are equally sensitive to changes in photophase light properties and, accordingly, prompt vigorous physiological responses, particularly allocating energy to functions related to survival during the stress exposure.

Urinary release of UMAdr and UMCort levels were expressed differently by the two species. In *M. socialis*, UMAdr and UMCort levels under long-wavelength light were 0.9- and 1.8-fold greater, respectively, than under short-wavelength light. By contrast, in *S. ehrenbergi*, the response was much larger, as the urinary metabolites levels under short-wavelength exposure were 2.6- and 4.1-fold greater, respectively. These results indicate that the HPA axis is more sensitive to photophase wavelength changes than the SAM system, as the response in the former pathway was the strongest in both species. According to the magnitudes of response in the two stress-response systems, it appears that *S. ehrenbergi* is more sensitive to changes in the photophase spectral composition than *M. socialis*. When compared with the HPA axis, the SAM system responds within seconds to stress but the activity quickly peaks and fades in response to a rapid negative feedback mechanism controlled by the parasympathetic nervous system (Ulrich-Lai and Herman, 2009). In contrast to the SAM system, HPA axis activation often peaks several minutes after the stress is terminated (Droste et al., 2008). The slower reaction of this axis reflects a pulsatile induction consisting of hierarchical, multifaceted neurohormonal signals (Lightman, 2008).

The intense stress response of *S. ehrenbergi* compared with that of *M. socialis* could simply reflect the differences in exposure to natural light between these two species. *M. socialis* is frequently exposed to surface illumination conditions as a result of its semi-fossorial lifestyle. By contrast, exposure to surface light conditions rarely occurs in *S. ehrenbergi* and typically only happens during a very brief period of time, as the animals would likely respond quickly by closing the breach in their dark environment.

Robust daily rhythms oscillating with 24-h τ were revealed in the present study in UMAdr and UMCort secretion in all experimental groups, except under the short-wavelength-exposed groups in which an ultradian rhythm of ~12-h τ was estimated by the spectral analysis. Although the circadian profile of adrenal activity seems to be SCN-driven (Kalsbeek et al., 2006; Ulrich-Lai

and Herman, 2009), a peripheral oscillator located within the adrenal gland has also been suggested to contribute to the gland's temporal organization (Sanyal et al., 1990; Dickmeis, 2009). Previous research has suggested that dual oscillator action mechanisms are responsible for reciprocal organization of the ultradian rhythms of rest and activity, with a semidian (12 h) periodicity (Broughton, 1985; Lloyd and Stupfel, 1991).

Daily rhythms in metabolic responses

VO_2 daily rhythms have been well documented in our laboratory for both species (Zubidat et al., 2007; Zubidat et al., 2010). It was revealed that they were significantly affected by LAN exposure and by photophase light with increasing intensity. In the present study, VO_2 rates exhibited a marked 24-h fluctuation in the short-wavelength-exposed groups of both species. Under long-wavelength exposure, both species displayed a compound rhythm oscillating with two harmonics of the 24-h rhythm (24 and 12 h) (Fig. 5). The prediction that energy consumption would correlate positively with locomotor activity has been underpinned by studies on several mammal and bird species (Bennett and Ruben, 1979; Taylor and Heglund, 1982; Taylor et al., 1982).

Recently, we have reported negative masking effects of increasing photophase irradiance on metabolic responses in these two species (Zubidat et al., 2010). It has been suggested that the irradiance-induced negative masking effects resulted from increased intervals of inactivity inside the underground burrows to maximize predator avoidance under the bright light conditions. In the present study, total DEE levels in *M. socialis* correlated positively with the photophase wavelength levels (Table 1), suggesting a negative masking effect on DEE by short-wavelength light. Similar masking effects of short-wavelength light have been documented previously (Thompson et al., 2008) in wild-type mice and were suggested to be mediated by cone photoreceptors that are sensitive to short-wavelength light. Additionally, the positive masking effect of DEE detected here in the long-wavelength-exposed *M. socialis* is expected to be regulated by the rod retinal photoreceptive system (Thompson et al., 2008). Negative masking of locomotion in response to short-wavelength light exposure would maximize the prospect of survival, e.g. hiding inside an underground shelter during the relatively intense light of day.

In contrast to *M. socialis*, total DEE levels in *S. ehrenbergi* were positively and negatively masked under the short- and long-wavelength light conditions, respectively. The novel photoreceptor melanopsin has been proposed as a potent co-mediator – with the classic photoreceptors (i.e. cones and rods) – of negative masking effects with long-wavelength light (Mrosovsky and Hattar, 2003; Thompson et al., 2008). Expression of melanopsin in the vestigial retina of *S. ehrenbergi* has been reported previously (Hannibal et al., 2002).

Conversely, positive masking reported here in *S. ehrenbergi* by the short-wavelength light cannot be explained by the involvement of melanopsin. First, the novel photopigment shows feeble and inadequate photosensitivity at short wavelengths (Panda et al., 2005; Mure et al., 2007). Second, mice lacking the classical cone and rod photoreceptors show impaired locomotion activity and nonresponsiveness to positive masking by light with varying spectral composition (Thompson et al., 2008; Mrosovsky et al., 1999). Thus, we suggest that the observed positive masking of the DEE rhythm in *S. ehrenbergi* by the short-wavelength light is mediated by rod and cone photoreceptors that are sensitive to short-wavelength light. Such photoreceptors, particularly rods that are sensitive to blue-shifted wavelength light, have been previously reported in *S. ehrenbergi* (Janssen et al., 2000; Janssen et al., 2003). Positive masking is postulated to enhance locomotor activity for exploring and seeking behavior when the animal is confronted with new surroundings or conditions (Mrosovsky et al., 2000). In the case of *S. ehrenbergi*, enhanced seeking behavior in response to a challenging light breach in the tunnel system (i.e. in order to seal it) would be beneficial to survival for this 'blind' subterranean species (Zuri and Terkel, 1999).

Conclusions

Light is an omnipresent stimulus with the prospect to act as a stressor. Recently, considerable research efforts have been devoted to study the adverse effect of visible light on human health and animal physiology and behavior (Navara and Nelson, 2007). Although light is obligatory for survival on earth, it could elicit several maladaptive responses when applied incongruously to biological systems. Here and in other recent studies (e.g. Zubidat et al., 2010), the differential stressful effects of photophase light with varying spectral composition (i.e. irradiance and wavelength) have been clearly demonstrated in two rodent species representing the extremes in their visual and ecological organization. The stress-induced responses of photophase light in the two species were associated with elevated metabolic responses, hypothetically to maintain homeostasis and thus facilitate individual survival. Finally, the retinal neural organization that mediates the differential physiological responses in *M. socialis* and *S. ehrenbergi* is equally multifaceted and has only recently been explored. Currently, a wide array of retinal photoreceptors expressing different light sensitivity is recognized as an important component regulating visual and temporal responses. In this regard, our results may be generalized to support the perception that classical and novel retinal photoreceptors are equally important for non-visual responses to environmental light signals and may play a significant role in the adaptation of rodents to various habitats.

LIST OF ABBREVIATIONS

6-SMT	6-sulfatoxymelatonin
DEE	daily energy expenditure
HPA	hypothalamic–pituitary–adrenocortical
IFPR	image-forming photoreceptor
LAN	light-at-night (exposure)
NIFPR	non-image-forming photoreceptor
PR	rhythm percentage
SAM	sympatho-adrenomedullary
SCN	suprachiasmatic nucleus
SD	short day
T_a	ambient temperature
UMAdr	urinary metabolites of adrenaline
UMCort	urinary metabolites of cortisol
VO_2	oxygen consumption

ACKNOWLEDGEMENTS

This study was supported by a granted from the United States–Israeli Binational Science Foundation (BSF) to A.H. and R.J.N.

REFERENCES

Aral, E., Uslu, S., Sunal, E., Sariboyaci, A. E., Okar, I. and Aral, E. (2006). Response of the pineal gland in rats exposed to three different light spectra of short periods. *Turk. J. Anim. Sci.* **30**, 29-34.

Arendt, J. (1985). Mammalian pineal rhythms. *Pineal Res. Rev.* **3**, 161-213.

Avivi, A., Oster, H., Joel, A., Beiles, A., Albrecht, U. and Nevo, E. (2004). Circadian genes in a blind subterranean mammal III: molecular cloning and circadian regulation of cryptochrome genes in the blind subterranean mole rat, *Spalax ehrenbergi* superspecies. *J. Biol. Rhythms* **19**, 22-34.

Banin, D., Haim, A. and Arad, Z. (1994). Metabolism and thermoregulation in the Levant vole *Microtus guentheri*: the role of photoperiodicity. *J. Therm. Biol.* **19**, 55-62.

Ben-Shlomo, R., Nevo, E., Ritte, U., Steinlechner, S. and Klante, G. (1996). 6-Sulphatoxymelatonin secretion in different locomotor activity types of the blind mole rat Spalax ehrenbergi. *J. Pineal Res.* **21**, 243-250.
Benjamini, L. (1989). Diel activity rhythms in the Levent vole, *Microtus guentheri*. *Isr. J. Zool.* **47**, 194-195.
Bennett, A. F. and Ruben, J. A. (1979). Endothermy and activity in vertebrates. *Science* **206**, 649-654.
Berson, D. M. (2007). Phototransduction in ganglion-cell photoreceptors. *Pflugers Arch.* **454**, 849-855.
Bingham, C., Arbogast, B., Guillaume, G. C., Lee, J. K. and Halberg, F. (1982). Inferential statistical methods for estimating and comparing cosinor parameters. *Chronobiologia* **9**, 397-439.
Broughton, R. J. (1985). Three central issues concerning ultradian rhythms. In *Ultradian Rhythms in Physiology and Behavior* (ed. H. Schulz and P. Lavie), pp. 217-233. New York: Springer-Verlag.
Bullough, J. D., Rea, M. S. and Figueiro, M. G. (2006). Of mice and women: light as a circadian stimulus in breast cancer research. *Cancer Causes Control* **17**, 375-383.
Cernuda-Cernuda, R., DeGrip, W. J., Cooper, H. M., Nevo, E. and García-Fernández, J. M. (2002). The retina of *Spalax ehrenbergi*: novel histologic features supportive of a modified photosensory role. *Invest. Ophthalmol. Vis. Sci.* **43**, 2374-2383.
Chávez, A. E., Bozinovic, F., Peichl, L. and Palacios, A. G. (2003). Retinal spectral sensitivity, fur coloration, and urine reflectance in the genus octodon (rodentia): implications for visual ecology. *Invest. Ophthalmol. Vis. Sci.* **44**, 2290-2296.
Cooper, H. M., Herbin, M. and Nevo, E. (1993). Visual system of a naturally microphthalmic mammal: the blind mole rat, *Spalax ehrenbergi*. *J. Comp. Neurol.* **328**, 313-350.
Daan, S. and Aschoff, J. (1982). Circadian contributions to survival. In *Vertebrate Circadian Rhythms* (ed. J. Aschoff, S. Daan and G. A. Groos), pp. 305-321. New York: Springer.
David-Gray, Z. K., Janssen, J. W., DeGrip, W. J., Nevo, E. and Foster, R. G. (1998). Light detection in a 'blind' mammal. *Nat. Neurosci.* **1**, 655-656.
Dickmeis, T. (2009). Glucocorticoids and the circadian clock. *J. Endocrinol.* **200**, 3-22.
Droste, S. K., de Groote, L., Atkinson, H. C., Lightman, S. L., Reul, J. M. and Linthorst, A. C. (2008). Corticosterone levels in the brain show a distinct ultradian rhythm but a delayed response to forced swim stress. *Endocrinology* **149**, 3244-3253.
Dunn, A. J. and Swiergiel, A. H. (2008). The role of corticotropin-releasing factor and noradrenaline in stress-related responses, and the inter-relationships between the two systems. *Eur. J. Pharmacol.* **583**, 186-193.
Gerkema, M. P., Groos, G. A. and Daan, S. (1990). Differential elimination of circadian and ultradian rhythmicity by hypothalamic lesions in the common vole, Microtus arvalis. *J. Biol. Rhythms* **5**, 81-95.
Goldman, B. D., Goldman, S. L., Riccio, A. P. and Terkel, J. (1997). Circadian patterns of locomotor activity and body temperature in blind mole-rats, *Spalax ehrenbergi*. *J. Biol. Rhythms* **12**, 348-361.
Goldstein, D. S. and Kopin, I. J. (2008). Adrenomedullary, adrenocortical, and sympathoneural responses to stressors: a meta-analysis. *Endocr. Regul.* **42**, 111-119.
Gouthiere, L., Mauvieux, B., Davenne, D. and Waterhouse, J. (2005). Complementary methodology in the analysis of rhythmic data, using examples from a complex situation, the rhythmicity of temperature in night shift workers. *Biol. Rhythm Res.* **36**, 177-193.
Graham, D. M., Wong, K. Y., Shapiro, P., Frederick, C., Pattabiraman, K. and Berson, D. M. (2008). Melanopsin ganglion cells use a membrane-associated rhabdomeric phototransduction cascade. *J. Neurophysiol.* **99**, 2522-2532.
Güler, A. D., Altimus, C. M., Ecker, J. L. and Hattar, S. (2007). Multiple photoreceptors contribute to nonimage-forming visual functions predominantly through melanopsin-containing retinal ganglion cells. *Cold Spring Harbor Symp. Quant. Biol.* **72**, 509-515.
Güler, A. D., Ecker, J. L., Lall, G. S., Haq, S., Altimus, C. M., Liao, H. W., Barnard, A. R., Cahill, H., Badea, T. C., Zhao, H. et al. (2008). Melanopsin cells are the principal conduits for rod-cone input to non-image-forming vision. *Nature* **453**, 102-105.
Haim, A., Heth, G., Pratt, H. and Nevo, E. (1983). Photoperiodic effects on thermoregulation in a 'blind' subterranean mammal. *J. Exp. Biol.* **107**, 59-64.
Haim, A., Zubidat, A. E. and Scantelbury, M. (2005). Seasonal and seasons out of time-thermoregulatory effects of light interference. *Chronobiol. Int.* **22**, 57-64.
Hankins, M. W., Peirson, S. N. and Foster, R. G. (2008). Melanopsin: an exciting photopigment. *Trends Neurosci.* **31**, 27-36.
Hannibal, J., Hindersson, P., Nevo, E. and Fahrenkrug, J. (2002). The circadian photopigment melanopsin is expressed in the blind subterranean mole rat, *Spalax*. *Neuroreport* **13**, 1411-1414.
Harrison, D. L. and Bates, P. J. (1991). *The Mammals of Arabia*, 2nd edn, pp. 309-313. Kent: Harrison Zoological Museum Publication.
Janssen, J. W., Bovee-Geurts, P. H., Peeters, Z. P., Bowmaker, J. K., Cooper, H. M., David-Gray, Z. K., Nevo, E. and DeGrip, W. J. (2000). A fully functional rod visual pigment in a blind mammal. A case for adaptive functional reorganization?. *J. Biol. Chem.* **275**, 38674-38679.
Janssen, J. W., David-Gray, Z. K., Bovee-Geurts, P. H., Nevo, E., Foster, R. G. and DeGrip, W. J. (2003). A green cone-like pigment in the 'blind' mole-rat Spalax ehrenbergi: functional expression and photochemical characterization. *Photochem. Photobiol. Sci.* **2**, 1287-1291.
Kalsbeek, A., Perreau-Lenz, S. and Buijs, R. M. (2006). A network of (autonomic) clock outputs. *Chronobiol. Int.* **23**, 201-215.
Kavakli, I. H. and Sancar, A. (2002). Circadian photoreception in humans and mice. *Mol. Interv.* **2**, 484-492.
Klerman, E. B., Shanahan, T. L., Brotman, D. J., Rimmer, D. W., Emens, J. S., Rizzo, J. F. and Czeisler, C. A. (2002). Photic resetting of the human circadian pacemaker in the absence of conscious vision. *J. Biol. Rhythms* **17**, 548-555.
Kumar, V. and Rani, S. (1999). Light sensitivity of the photoperiodic response system in higher vertebrates: wavelength and intensity effects. *Indian J. Exp. Biol.* **37**, 1053-1064.
Lightman, S. L. (2008). The neuroendocrinology of stress: a never ending story. *J. Neuroendocrinol.* **20**, 880-884.
Lloyd, D. and Stupfel, M. (1991). The occurrence and functions of ultradian rhythms. *Biol. Rev. Camb. Philos. Soc.* **66**, 275-299.
Lucas, R. J., Freedman, M. S., Munoz, M., Garcia-Fernandez, J. M. and Foster, R. G. (1999). Regulation of the mammalian pineal by non-rod, non-cone, ocular photoreceptors. *Science* **284**, 505-507.
Mrosovsky, N. and Hattar, S. (2003). Impaired masking responses to light in melanopsin-knockout mice. *Chronobiol. Int.* **20**, 989-999.
Mrosovsky, N., Foster, R. G. and Salmon, P. A. (1999). Thresholds for masking responses to light in three strains of retinally degenerate mice. *J. Comp. Physiol. A* **184**, 423-428.
Mrosovsky, N., Salmon, P. A., Foster, R. G. and McCall, M. A. (2000). Responses to light after retinal degenerationn. *Vision Res.* **40**, 575-578.
Mure, L. S., Rieux, C., Hattar, S. and Cooper, H. M. (2007). Melanopsin-dependent nonvisual responses: evidence for photopigment bistability in vivo. *J. Biol. Rhythms* **22**, 411-424.
Nakahara, D., Nakamura, M., Iigo, M. and Okamura, H. (2003). Bimodal circadian secretion of melatonin from the pineal gland in a living CBA mouse. *Proc. Natl. Acad. Sci. USA* **100**, 9584-9589.
Navara, K. J. and Nelson, R. J. (2007). The dark side of light at night: physiological, epidemiological, and ecological consequences. *J. Pineal Res.* **43**, 215-224.
Nelson, W., Tong, Y., Lee, J. and Halberg, F. (1979). Methods for cosinor-rhythmometry. *Chronobiologia* **6**, 305-323.
Nevo, E. (1999). *Mosaic Evolution of Subterranean Mammals: Regression, Progression and Global Convergence*. Oxford: Oxford University Press.
Nevo, E., Ivanitskaya, E. and Beiles, A. (2001). *Adaptive Radiation of Blind Subterranean Mole Rats*. Leiden, Netherlands: Backhuys.
Panda, S., Nayak, S. K., Campo, B., Walker, J. R., Hogenesch, J. B. and Jegla, T. (2005). Illumination of the melanopsin signaling pathway. *Science* **307**, 600-604.
Pandi-Perumal, S. R., Trakht, I., Srinivasan, V., Spence, D. W., Maestroni, G. J., Zisapel, N. and Cardinali, D. P. (2008). Physiological effects of melatonin: role of melatonin receptors and signal transduction pathways. *Prog. Neurobiol.* **85**, 335-353.
Peichl, L. (2005). Diversity of mammalian photoreceptor properties: adaptations to habitat and lifestyle? *Anat. Rec. A Discov. Mol. Cell. Evol. Biol.* **287**, 1001-1012.
Pévet, P., Agez, L., Bothorel, B., Saboureau, M., Gauer, F., Laurent, V. and Masson-Pévet, M. (2006). Melatonin in the multi-oscillatory mammalian circadian world. *Chronobiol. Int.* **23**, 39-51.
Rado, R., Gev, H., Goldamn, B. D. and Terkel, J. (1991). Light and circadian activity in the blind mole rat. In *Photobiology* (ed. E. Riklis), pp. 581-589. New York: Plenum.
Refinetti, R., Cornélissen, G. and Halberg, F. (2007). Procedures for numerical analysis of circadian rhythms. *Biol. Rhythm Res.* **38**, 275-325.
Reiter, R. J. (1994). Non-visible electromagnetic radiation and pineal function. Eye-Pineal Relationships International Symposium, Nencki Institute Warszawa. *Acta Neurobiol. Exp.* **54**, 93-94.
Sanyal, S., Jansen, H. G., de Grip, W. J., Nevo, E. and de Jong, W. W. (1990). The eye of the blind mole rat, *Spalax ehrenbergi*. Rudiment with hidden function? *Invest. Ophthalmol. Vis. Sci.* **31**, 1398-1404.
Speakman, J. (2000). The cost of living: field metabolic rates of small mammals. *Adv. Ecol. Res.* **30**, 177-297.
Taylor, C. R. and Heglund, N. C. (1982). Energetics and mechanics of terrestrial locomotion. *Annu. Rev. Physiol.* **44**, 97-107.
Taylor, C. R., Heglund, N. C. and Maloiy, G. M. (1982). Energetics and mechanics of terrestrial locomotion. I. Metabolic energy consumption as a function of speed and body size in birds and mammals. *J. Exp. Biol.* **97**, 1-21.
Tendron-Franzin, A., Gouyon, J. B., Guignard, J. P., Decramer, S., Justrabo, E., Gilbert, T. and Semama, D. S. (2004). Long-term effects of in utero exposure to cyclosporin A on renal function in the rabbit. *J. Am. Soc. Nephrol.* **15**, 2687-2693.
Thompson, S., Foster, R. G., Stone, E. M., Sheffield, V. C. and Mrosovsky, N. (2008). Classical and melanopsin photoreception in irradiance detection: negative masking of locomotor activity by light. *Eur. J. Neurosci.* **27**, 1973-1979.
Ulrich-Lai, Y. M. and Herman, J. P. (2009). Neural regulation of endocrine and autonomic stress responses. *Nat. Rev. Neurosci.* **10**, 397-409.
Van Gelder, R. N. (2005). Nonvisual ocular photoreception in the mammal. *Methods Enzymol.* **393**, 746-755.
Wehr, T. A., Schwartz, P. J., Turner, E. H., Feldman-Naim, S., Drake, C. L. and Rosenthal, N. E. (1995). Bimodal patterns of human melatonin secretion consistent with a two-oscillator model of regulation. *Neurosci. Lett.* **194**, 105-108.
Zawilska, J. B., Skene, D. J. and Arendt, J. (2009). Physiology and pharmacology of melatonin in relation to biological rhythms. *Pharmacol. Rep.* **61**, 383-410.
Zubidat, A. E. and Haim, A. (2007). The effect of alpha- and beta-adrenergic blockade on daily rhythms of body temperature, urine production, and urinary 6-sulfatoxymelatonin of social voles *Microtus socialis*. *Comp. Biochem. Physiol. A Mol. Integr. Physiol.* **148**, 301-307.
Zubidat, A. E., Ben-Shlomo, R. and Haim, A. (2007). Thermoregulatory and endocrine responses to light pulses in short-day acclimated *M. socialis* (*Microtus socialis*). *Chronobiol. Int.* **24**, 269-288.
Zubidat, A. E., Nelson, R. J. and Haim, A. (2008). Urinary adrenalin and cortisol secretion patterns of *M. socialis* in response to adrenergic blockade under basal conditions. *Physiol. Behav.* **93**, 243-249.
Zubidat, A. E., Nelson, R. J. and Haim, A. (2009). Photosensitivity to different light intensities in blind and sighted rodents. *J. Exp. Biol.* **212**, 3857-3864.
Zubidat, A. E., Nelson, R. J. and Haim, A. (2010). Differential effects of photophase irradiance on metabolic and urinary stress hormone concentrations in 'blind' and sighted rodents. *Chronobiol. Int.* **27**, 487-516.
Zuri, I. and Terkel, J. (1996). Locomotor patterns, territory, and tunnel utilization in the mole-rat *Spalax ehrenbergi*. *J. Zool.* **240**, 123-140.

Table S1. Factorial and cosinor analyses of urine production rates in two rodent species, *Microtus socialis* and *Spalax ehrenbergi*, under different light spectra

	One-way ANOVA ($F_{6,42}$; P)	τ (h)	Mesor (ml 100g^{-1} h^{-1})	Amplitude (ml 100g^{-1} h^{-1})	Acrophase (hh:mm)	PR (%)	$F_{2,6}$; P
M. socialis							
Short wavelength	1.12; 0.37	24	0.66 (0.59–0.74)[a]	0.28 (0.22–0.34)	23:40 (21:40–01:36)	70	79.91; 0.0001
Long wavelength	1.05; 0.47	24	0.26[b]	0.12	00:16	9	8.36; 0.08
S. ehrenbergi							
Short wavelength	66.79; 0.0001	24	0.98 (0.88–1.07)	0.43 (0.29–0.57)	01:18 (00:10–02:28)[a]	59	16.46; 0.004
Long wavelength	5.25; 0.001	12	0.95 (0.83–1.07)	0.32 (0.15–0.51)	00:12 (00:01–00:37)[b]	54	32.12; 0.03

τ, period length of the cosine curve approximated by spectral analysis; PR, percentage of the rhythm (represents the proportion of the total variance of the data accounted by the cosine approximation of a trial period).

The zero amplitude hypothesis was rejected at $P<0.05$. Different letters represent significant differences between treatments for each species ($P<0.05$).

Values in brackets for mesor, amplitude and acrophase are 95% confidence intervals (CI) of the group mean. CI values are not listed when $P>0.05$.

Table S2. Factorial and cosinor analyses of urinary 6-sulfatoxymelatonin (6-SMT) in two rodent species, *Microtus socialis* and *Spalax ehrenbergi*, under different light spectra

	One-way ANOVA ($F_{6,36}$; P)	τ (h)	Mesor (ng ml^{-1})	Amplitude (ng ml^{-1})	Acrophase (hh:mm)	PR (%)	$F_{2,5}$; P
M. socialis							
Short wavelength	19.42; 0.0001	24	3.70 (3.28–4.11)[a]	1.84 (1.23–2.64)[a]	02:49 (01:38–03:59)[a]	68	31.63; 0.001
Long wavelength	1.66; 0.16	8	1.72 (1.45–2.02)[b]	0.49 (0.05–1.12)[b]	06:58 (05:59–08:31)[b]	48	6.70; 0.03
S. ehrenbergi							
Short wavelength	5.05; 0.001	24	1.32 (1.15–1.51)[a]	0.51 (0.25–0.77)[a]	19:04 (16:52–21:20)[a]	61	6.66; 0.04
Long wavelength	9.72; 0.0001	12	3.38 (3.04–3.72)[b]	1.59 (1.13–2.04)[b]	01:48 (00:52–02:44)[b]	66	21.61; 0.004

τ, period length of the cosine curve approximated by spectral analysis; PR, percentage of the rhythm (represents the proportion of the total variance of the data accounted by the cosine approximation of a trial period).

The zero amplitude hypothesis was rejected at $P<0.05$. Different letters represent significant differences between treatments for each species ($P<0.05$).

Values in brackets for mesor, amplitude and acrophase are 95% confidence intervals (CI) of the group mean.

Table S3. Factorial and cosinor analyses of urinary metabolites of adrenaline (UMAdr) in two rodent species, *Microtus socialis* and *Spalax ehrenbergi*, under different light spectra

	One-way ANOVA ($F_{6,36}$; P)	τ (h)	Mesor (pg ml^{-1} g^{-1})	Amplitude (pg ml^{-1} g^{-1})	Acrophase (hh:mm)	PR (%)	$F_{2,5}$; P
M. socialis							
Short wavelength	8.19; 0.0001	24	180 (161–199)[a]	34.7 (13.7–57.5)[a]	17:28 (15:04–19:56)[a]	48	13.72; 0.01
Long wavelength	12.35; 0.0001	24	27 (240–303)[b]	108 (65.6–151)[b]	21:32 (19:52–23:12)[b]	58	36.92; 0.001
S. ehrenbergi							
Short wavelength	2.72; 0.03	24	181 (132–230)[a]	27.5 (10.0–44.9)	18:10 (14:12–22:08)	24	13.10; 0.02
		8		40.4 (31.5–49.3)	03:44 (00:46–06:12)	39	57.46; 0.001
Long wavelength	2.10; 0.04	24	69.1 (56.1–82.1)[b]	23.2 (3.68–42.6)	14:32 (10:56–18:08)	66	7.28; 0.04

τ, period length of the cosine curve approximated by spectral analysis; PR, percentage of the rhythm (represents the proportion of the total variance of the data accounted by the cosine approximation of a trial period).

The zero amplitude hypothesis was rejected at $P<0.05$. Different letters represent significant differences between treatments for each species ($P<0.05$).

Values in brackets for mesor, amplitude and acrophase are 95% confidence intervals (CI) of the group mean.

Table S4. Factorial and cosinor analyses of urinary metabolites of cortisol (UMCort) in two rodent species, *Microtus socialis* and *Spalax ehrenbergi*, under different light spectra

	One-way ANOVA ($F_{6,36}$; P)	τ (h)	Mesor (pg ml^{-1} g^{-1})	Amplitude (pg ml^{-1} g^{-1})	Acrophase (hh:mm)	PR (%)	$F_{2,5}$;P
M. socialis							
Short wavelength	0.1; 0.44	12.9	33.4 (27.3–39.5)[a]	6.31 (1.95–14.6)	08:02 (05:55–10:08)	49	9.37; 0.04
Long wavelength	5.34; 0.0001	24	59.4 (51.4–67.4)[b]	20.4 (9.37–31.3)	10:04 (07:48–12:24)	43	11.68; 0.01
S. ehrenbergi							
Short wavelength	0.18; 0.98	12	49.0	1.56	08:58	37	0.17; 0.84
Long wavelength	6.39; 0.0001	24	11.5 (9.24–13.8)	4.89 (1.46–8.32)	02:39 (00:06–05:24)	43	10.42; 0.02

τ, period length of the cosine curve approximated by spectral analysis; PR, percentage of the rhythm (represents the proportion of the total variance of the data accounted by the cosine approximation of a trial period).

The zero amplitude hypothesis was rejected at $P<0.05$. Different letters represent significant differences between treatments for each species ($P<0.05$).

Values in brackets for mesor, amplitude and acrophase are 95% confidence intervals (CI) of the group mean. CI values are not listed when $P>0.05$.

Table S5. Factorial and cosinor analyses of daily rhythms in oxygen consumption (VO_2) of two rodent species, *Microtus socialis* and *Spalax ehrenbergi*, under different light spectra

	One-way ANOVA ($F_{48,336}$; P)	τ (h)	Mesor (ml 100 g^{-1} h^{-1})	Amplitude (ml 100 g^{-1} h^{-1})	Acrophase (hh:mm)	PR (%)	$F_{2,6}$; P
M. socialis							
Short wavelength	2.27; 0.0001	24	1.84 (1.81–1.87)[a]	0.16 (0.11–0.20)[a]	19:44 (18:36–20:52)[a]	73	4.75; 0.001
Long wavelength	3.98; 0.02	24	2.72 (2.64–2.80)[b]	0.37 (0.25–0.48)[b]	20:36 (18:20–20:52)[a]	43	4.04; 0.04
		12		0.25 (0.08–0.32)[a]	07:06 (05:52–08:20)[b]	23	9.11; 0.01
S. ehrenbergi							
Short wavelength	4.03; 0.02	24	3.13 (3.07–3.19)[a]	0.30 (0.22–0.39)[a]	05:46 (04:39–06:52)[a]	45	7.02; 0.001
Long wavelength	2.42; 0.04	24	1.92 (1.81–2.02)[c]	0.52 (0.37–0.66)[b]	04:38 (03:33–05:44)[a]	30	2.44; 0.001
		12		0.39 (0.24–0.53)[a,b]	03:50 (03:04–04:34)[b]	22	2.10; 0.001

τ, period length of the cosine curve approximated by spectral analysis; PR, percentage of the rhythm (represents the proportion of the total variance of the data accounted by the cosine approximation of a trial period).

The zero amplitude hypothesis was rejected at $P<0.05$. Different letters represent significant differences between treatments for each species ($P<0.05$).

Values in brackets for mesor, amplitude and acrophase are 95% confidence intervals of the group mean.